International Journal of Power Electronics and Drive System (IJPEDS)
Vol. 6, No. 1, March 2015, pp. 32~44
ISSN: 2088-8694

A Comparison Between Two Average Modelling Techniques of AC-AC Power Converters

Paweł Szcześniak
Institute of Electrical Engineering, University of Zielona Góra, Podgorn, Poland

Article Info

Article history:

Received Sep 22, 2014
Revised Dec 4, 2014
Accepted Dec 21, 2014

Keyword:

Averaged model
Buck-boost topology
Matrix converter
Modelling
Power converters

ABSTRACT

In this paper, a comparative evaluation of two modelling tools for switching AC-AC power converters is presented. Both of them are based on average modelling techniques. The first approach is based on the circuit averaging technique and consists in the topological manipulations, applied to a converter states. The second approach makes use of a state-space averaged model of the converter and is based on analytical manipulations using the different state representations of a converter. The two modelling techniques are applied to a same AC-AC called matrix-reactance frequency converter based on buck-boost topology. These techniques are compared on the basis of their rapidity, quantity of calculations and transformations and its limitations.

Corresponding Author:

Paweł Szcześniak,
Institute of Electrical Engineering,
University of Zielona Gora,
65-246 Zielona Góra, Podgorn1 50, Poland.
Email: P.Szczesniak@iee.uz.zgora.pl

1. INTRODUCTION

Modelling a power electronic converter is a complex issue due to the fact of digital control complexity and high number of power converter components. Furthermore, given the increasing number of different modulation strategies, it is necessary to study their impact in converter operation. In order to achieve their goal power converters must be appropriately modelled in simulation or analytical studies. Hence it is necessary to create simple models. The problem has been largely studied and a wide variety of models have been proposed [1]-[6]. However, the use of those models and their simulation in a computer still requires a large amount of resources and circuit simplification and mathematical transformations. In this paper, a comparative evaluation of two modelling approach of complex direct AC-AC frequency converters is presented. The presented modelling methods are based on circuit averaging technique [1], [5] and state-space averaged model [5].

The change of frequency in AC voltage is now one of the important functions of solid state power converters. The most desirable features of frequency converters include the possibility of generating load voltages with arbitrary amplitude and generating sinusoidal source and load currents and voltage waveforms, the possibility of providing unity power factor for any load, and finally, their construction using a simple and compact power circuit. The past few years have witnessed remarkable progress in research into direct power AC–AC frequency converters without a DC energy storage element. Many exciting applications have been developed [7]-[12]. The most common is the matrix converter (MC) topology [7]. Another group of AC–AC frequency converters with a buck–boost voltage transformation possibility and without DC energy storage is proposed in [10]-[12], and are known as matrix-reactance frequency converters (MRFC). The expected benefit of these converters is the voltage transfer ratio which is much greater than one and depends on reactive elements [12].

The analysis and modelling of MRFC presents significant challenges, due to their discontinuous switching behavior and the increasing number of different modulation strategies [13]. It is necessary to study the modulation process impact in converter operation.

The main aim of this paper is to present two mathematical models of the selected topologies of MRFCs with simple Venturini modulation [13]. The results of the study and mathematical analysis presented in this paper are based on the previously presented results presented in [14]-[16]. One well-known approach to the modelling of power converters is to approximate their operation using averaging techniques [1]. The generalized averaging method is based on the fact that the waveforms can be approximated using a defined time interval, which is determined by a switching sequence period T_{Seq}. Initially, the average method was widely used for DC–DC converter modelling [1]. Then it was applied to other types of converters: [2]-[6]. As a main achievement of the paper is to show the differences in the results of two analyzed modelling methods, which are summarized in the section 4.

2. DESCRIPTION OF THE ANALYZED MATRIX-REACTANCE FREQUENCY CONVERTER

The family of MCRFCs contains 9 topologies - two topologies based on buck-boost, Ćuk, SEPIC and Zeta topologies and one based on the boost topology [10], [12]. First an MRFC based on buck-boost topology (MRFC-I-buck-boost), shown in Fig. 1, will be analyzed [10]. The descriptions, in general form, of the control strategy of the discussed MRFCs is shown in Figure 2 [12]. Each sequence period is divided into two parts t_S and t_L. Time t_S is related to matrix connected switch sets operations. In each switching cycle T_{Seq}, in the interval t_S, the matrix connected switch sets are in the process of switching with selected switching modulation, while the load synchronous connected switch sets are turned-off. The voltages u_a, u_b, u_c are formed by setting the requested output frequency f_L, with sequential piecewise sections of the input voltage waveforms u_A, u_B, u_C. At the same time the electrical energy is stored in the inductor L_{S1}, L_{S2}, L_{S3}. In contrast, in the time period t_L all of the matrix connected switch sets (MCS) are turned-off and the load synchronous connected switch sets are turned-on. The energy stored in source inductors L_{S1}, L_{S2}, L_{S3} is transferred to the load capacitor C_{L1}, C_{L2}, C_{L3}. In this way, we obtain the possibility of increasing the output voltage. The duty factors of load switches depend on the expected output voltages.

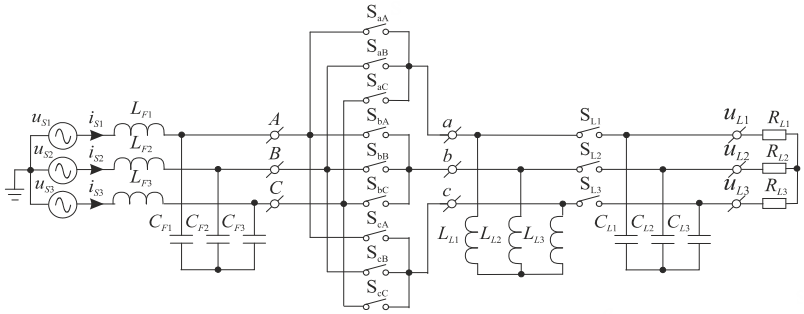

Figure 1. Topology of matrix-reactance frequency converter based on buck–boost topology (MRFC-I-buck-boost) [10], [12]

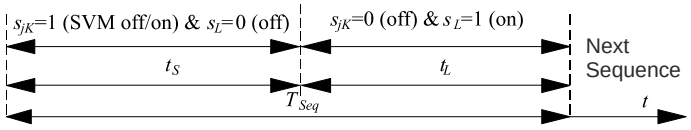

Figure 2. General form of the control strategy

The state of the converter switches can be represented by means of the so-called transfer matrix **T** (1), (2). The matrix **T** is defined by using modulation strategy of matrix connected switch sets, and describes the low frequency input to output current and voltages relationships [12].

$$\begin{bmatrix} u_a(t) \\ u_b(t) \\ u_c(t) \end{bmatrix} = \begin{bmatrix} s_{aA}(t) & s_{aB}(t) & s_{aC}(t) \\ s_{bA}(t) & s_{bB}(t) & s_{bC}(t) \\ s_{cA}(t) & s_{cB}(t) & s_{cC}(t) \end{bmatrix} \begin{bmatrix} u_A(t) \\ u_B(t) \\ u_C(t) \end{bmatrix} = \mathbf{T}\mathbf{u}_S \,, \tag{1}$$

$$\begin{bmatrix} i_A(t) \\ i_B(t) \\ i_C(t) \end{bmatrix} = \begin{bmatrix} s_{aA}(t) & s_{bA}(t) & s_{cA}(t) \\ s_{aB}(t) & s_{bB}(t) & s_{cB}(t) \\ s_{aC}(t) & s_{bC}(t) & s_{cC}(t) \end{bmatrix} \begin{bmatrix} i_a(t) \\ i_b(t) \\ i_c(t) \end{bmatrix} = \mathbf{T}^T \mathbf{i}_L \,. \tag{2}$$

Where: s_{jK} -switch state function, $j = \{a, b, c\}$, $K = \{A, B, C\}$ –names of input and output phases. The MCS work with a high switching frequency. A low frequency load voltage of variable amplitude and frequency can be generated by modulating the duty cycle of the switches using their respective switching functions s_{jK}. A modulation duty cycle should be defined for each switch in order to determine the average behaviour of the MCS output voltage waveform [12], [13]. The modulation duty cycle is defined by:

$$d_{jK}(t) = \frac{t_{jK}}{T_{Seq}} \tag{3}$$

Where t_{jK} represents the time when switch S_{jK} is turned on and T_{Seq} represents the time of the complete sequence in the PWM pattern, and $0 < d_{jK} < 1$. Based on the switch duty-ratios, the averaged output voltages and the averaged input currents can be related to the input voltages and the output currents, respectively, as:

$$\bar{\mathbf{u}}_L(t) = \mathbf{M}(t)\bar{\mathbf{u}}_S \,, \qquad \bar{\mathbf{i}}_S(t) = \mathbf{M}^T(t)\bar{\mathbf{i}}_L \,, \tag{4}$$

$$\mathbf{M}(t) = \begin{bmatrix} d_{aA} & d_{aB} & d_{aC} \\ d_{bA} & d_{bB} & d_{bC} \\ d_{cA} & d_{cB} & d_{cC} \end{bmatrix} . \tag{5}$$

The classical Venturini control strategy is taking into consideration with low frequency transfer matrix described by (5) [13]. Taking into account limited switching time t_S of MCS, the modulation duty cycles d_{jK} for MRFC-I-buck-boost are defined by (6) and (7) [12]. Exemplary time waveforms of the control signals, illustrating operation of the discussed MRFC is shown in Figure 3.

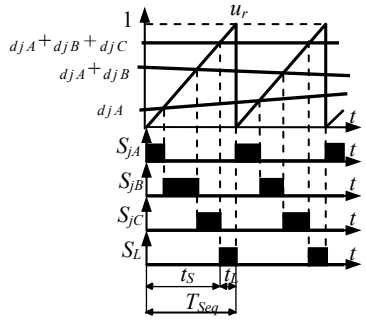

Figure 3. Exemplary time waveforms of the control signals in MRFC-I-buck-boost for switches in one phase

$$\begin{aligned} d_{aA} &= d_{bB} = d_{cC} = D_S(1 + 2q\cos(\omega_m t + \varphi))/3 \\ d_{aB} &= d_{cA} = d_{bC} = D_S(1 + 2q\cos(\omega_m t + \varphi - 2\pi/3))/3 \,, \\ d_{aC} &= d_{bA} = d_{cB} = D_S(1 + 2q\cos(\omega_m t + \varphi - 4\pi/3))/3 \end{aligned} \tag{6}$$

$$D_S = \frac{t_S}{T_{Seq}} \,, \tag{7}$$

Where: $\omega_m = \omega_L - \omega$, ω, ω_L – pulsation of the supply and load voltages respectively, D_S –sequence pulse duty factor, q– voltage gain ($0 \le q \le 0.5$).

The matrix $\mathbf{M}(t)$ is known as the modulation matrix or low-frequency transfer matrix. Based on these relationships in (4) and (5), a matrix converter on a switching-cycle averaged basis can be represented by nine ideal transformers with varying turn-ratios, as shown in Figure 4(a), whereas output switches can be represented by ideal transformers with turn-ratios equal 1-D_S, as shown in Figure 4(b) [12].

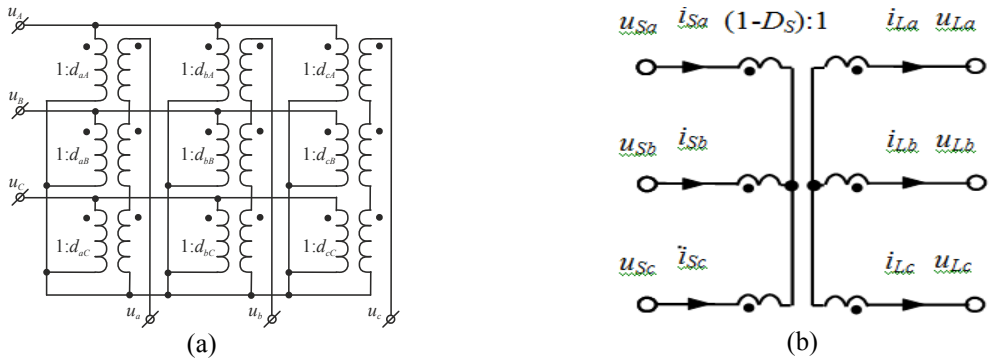

Figure 4. Averaged-switching-cycle representation: a) matrix connected switches (MCS), b) load switches

3. AVERAGE MODELLING TECHNIQUES

Average modelling techniques are based principally on replacing all currents and voltages of the system by their mean value over a switching period and ignoring thus their high frequency components. The local average of function $d(t)$ is defined as follows [4]:

$$d(t) = \frac{1}{T_{Seq}} \int_{t-T_{Seq}}^{t} q(\tau) d\tau \,, \tag{8}$$

Where $d(t)$ is the continuous duty factor. For the next sequence periods T_{Seq} becomes $d(kT_{Seq})=d_k(t)$, where $d_k(t)$ is the actual duty factor in the *k-th* cycle. If function $d(t)$ is periodic with period T_{Seq}, then $d(t)=D$ where D is the steady-state duty ratio [4].

There are among others two presented in this paper strategies used for the derivation of the averaged model: circuit average technique and state-space averaging technique.

3.1. Circuit Averaging Technique

Sinusoidal time-varying systems can be changed to time-invariant system by the $dq0$ transformation [2], [14]-[18]. The $dq0$ transformation of the variables is given as follows:

$$\mathbf{x}_{dq0} = \mathbf{K}\mathbf{x}_{abc}, \quad \mathbf{x}_{abc} = \mathbf{K}^{-1}\mathbf{x}_{dq0}, \tag{9}$$

Where: $x_{abc}=[x_a, x_b, x_c]^T$, $x_{dq0}=[x_q, x_d, x_0]$T, x_d- forward (rotating) phasor, x_q- backward (rotating) phasor, x_0- zero-sequence component [2],

$$\mathbf{K} = \begin{bmatrix} \mathbf{K}_S & \cdots & 0 \\ \vdots & \ddots & \vdots \\ 0 & \cdots & \mathbf{K}_L \end{bmatrix}, \tag{10}$$

$$\mathbf{K}_S = \sqrt{\frac{2}{3}} \begin{bmatrix} \cos(\omega t) & \sin(\omega t) & 1/\sqrt{2} \\ \cos(\omega t - 2\pi/3) & \sin(\omega t - 2\pi/3) & 1/\sqrt{2} \\ \cos(\omega t + 2\pi/3) & \sin(\omega t + 2\pi/3) & 1/\sqrt{2} \end{bmatrix}, \tag{11}$$

$$\mathbf{K}_L = \sqrt{\frac{2}{3}}\begin{bmatrix} \cos(\omega_L t) & \sin(\omega_L t) & 1/\sqrt{2} \\ \cos(\omega_L t - 2\pi/3) & \sin(\omega_L t - 2\pi/3) & 1/\sqrt{2} \\ \cos(\omega_L t + 2\pi/3) & \sin(\omega_L t + 2\pi/3) & 1/\sqrt{2} \end{bmatrix}, \quad (12)$$

Where: $\mathbf{K}_S$ and $\mathbf{K}_L$ are the $dq0$ transformation matrices defined for pulsation of the supply and load voltages, ω and ω_L respectively [14], [16].

The circuit $dq0$ transformation is obtained by the following procedures [14]:

a) Partition of the averaged circuit model into basic subcircuits.

b) Transformation of each of the subcircuits into $dq0$ equivalent circuits based on the $dq0$ transformation equations.

3.1.1. Partition of the Circuit into Basic Subcircuits

We can divide the averaged circuit model of the presented MRFC into several fundamental subcircuits along the dotted lines indicated in Figure 5. After partitioning, we obtain eight basic subcircuits.

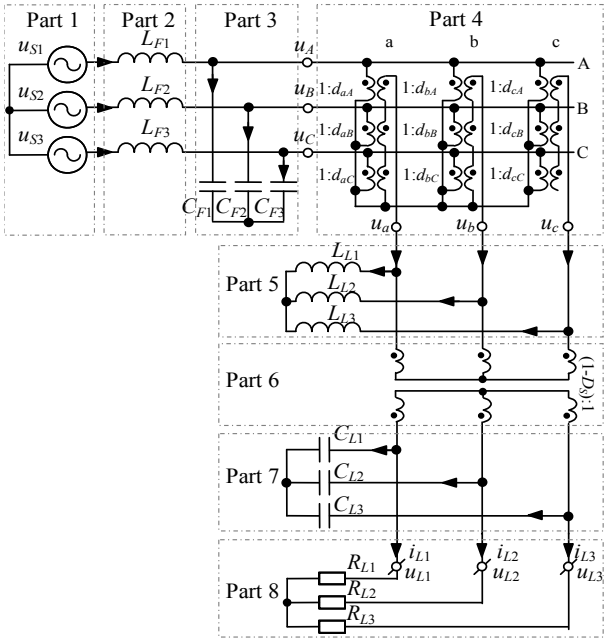

Figure 5. Averaged circuit model of the considered MRFC

3.1.2. Transformation of Basic Subcircuits into dq0 Equivalent Circuits

For a three-phase balanced voltage source set (Part 1), the procedure is as follows [2]-[3], [14]:

$$\mathbf{u}_{Sdq0} = \mathbf{K}_S \mathbf{u}_S = \mathbf{K}_S U_S \begin{bmatrix} \sin(\omega t + \varphi_1) \\ \sin(\omega t - 2\pi/3 + \varphi_1) \\ \sin(\omega t + 2\pi/3 + \varphi_1) \end{bmatrix} = U_S \begin{bmatrix} \sin\varphi_1 \\ \cos\varphi_1 \\ 0 \end{bmatrix} \quad (13)$$

Where $\mathbf{u}_S$ is the vector of the voltage sources. Thus, the $dq0$ transformed circuits of the voltage source set is shown in Fig. 6a. Using basic principles from circuit theory, the source inductors (Part 2) are modelled by Equation (14) [2], [14]:

$$L_F \frac{d\,\mathbf{i}_{LFabc}}{dt} = \mathbf{u}_{LFabc} \quad (14)$$

Where $L_{F1}=L_{F2}=L_{F3}=L_F$. Application of (9) to (14) yields:

$$L_F\left(\frac{d\,\mathbf{K}_S^{-1}}{dt}\mathbf{i}_{LFdq0}+\mathbf{K}_S^{-1}\frac{d\,\mathbf{i}_{LFdq0}}{dt}\right)=\mathbf{u}_{LFabc} \tag{15}$$

Finally, the *dq*0 transform of source inductors can be formulated as:

$$L_F\frac{d\,\mathbf{i}_{LFdq0}}{dt}=-L_F\mathbf{K}_S\frac{d\,\mathbf{K}_S^{-1}}{dt}\mathbf{i}_{LFdq0}+\mathbf{K}_S\mathbf{u}_{LFdq0}=-L_F\omega\begin{bmatrix}0&1&0\\-1&0&0\\0&0&0\end{bmatrix}\mathbf{i}_{LFdq0}+\mathbf{u}_{LFdq0} \tag{16}$$

And the circuit models are shown in Figure 6(b). The *dq*0 "inductor" is represented by real dynamic inductor L_F in series with an imaginary static reactor $\pm j\omega L_F$. Since the voltage and current of the static reactor obeys Ohm's law, the reactor is replaced by a lossless resistor symbol [2].

Similar, equations and circuit models apply to the load inductor set (Part 5):

$$L_L\frac{d\,\mathbf{i}_{LLabc}}{dt}=\mathbf{u}_{LLabc} \tag{17}$$

Where $L_{L1}=L_{L2}=L_{L3}=L_L$. From expression (9), (12), and (17) obtain:

$$L_L\frac{d\,\mathbf{i}_{LLdq0}}{dt}=-L_L\mathbf{K}_L\frac{d\,\mathbf{K}_L^{-1}}{dt}\mathbf{i}_{LLdq0}+\mathbf{K}_L\mathbf{u}_{LLdq0}=-L_L\omega_L\begin{bmatrix}0&1&0\\-1&0&0\\0&0&0\end{bmatrix}\mathbf{i}_{LLdq0}+\mathbf{u}_{LLdq0} \tag{18}$$

Figure 6(c) illustrates the *dq*0 components of load inductors. For the source capacitors circuit (Part 3), the differential equations are in the following form [2], [14]:

$$C_F\frac{d\,\mathbf{u}_{CFabc}}{dt}=\mathbf{i}_{CFabc} \tag{19}$$

Where $C_{F1}=C_{F2}=C_{F3}=C_F$. Taking into account expressions (9), (11) and (19), the *dq*0 transform of source capacitors is defined as follows:

$$C_F\left(\frac{d\,\mathbf{K}_S^{-1}}{dt}\mathbf{u}_{CFdq0}+\mathbf{K}_S^{-1}\frac{d\,\mathbf{u}_{CFdq0}}{dt}\right)=\mathbf{i}_{CFabc} \tag{20}$$

$$C_F\frac{d\,\mathbf{u}_{CFdq0}}{dt}=-C_F\mathbf{K}_S\frac{d\,\mathbf{K}_S^{-1}}{dt}\mathbf{u}_{CFdq0}+\mathbf{K}_S\mathbf{i}_{CFdq0}=-C_F\omega\begin{bmatrix}0&1&0\\-1&0&0\\0&0&0\end{bmatrix}\mathbf{u}_{CFdq0}+\mathbf{i}_{CFdq0} \tag{21}$$

For the load capacitors circuit (Part 7), the *dq*0 transform is defined as follows:

$$C_L\frac{d\,\mathbf{u}_{CLabc}}{dt}=\mathbf{i}_{CLabc} \tag{22}$$

$$C_L\frac{d\,\mathbf{u}_{CLdq0}}{dt}=-C_L\mathbf{K}_L\frac{d\,\mathbf{K}_L^{-1}}{dt}\mathbf{u}_{CLdq0}+\mathbf{K}_L\mathbf{i}_{CLdq0}=-C_L\omega_L\begin{bmatrix}0&1&0\\-1&0&0\\0&0&0\end{bmatrix}\mathbf{u}_{CLdq0}+\mathbf{i}_{CLdq0} \tag{23}$$

The *dq*0 transformed circuit of source and load capacitor sets are shown in Figure 6(d) and Figure 6(e), respectively. Similar as with inductors, the *dq*0 "capacitors" are represented by real dynamic capacitors C_F and C_L in parallel with imaginary static reactors $\pm 1/(j\omega C_F)$, and $\pm 1/(j\omega_L C_L)$ [2]. If the switching

function of the matrix switches is defined by (4)-(7) then the *dq*0 transformation of the MCS (Part 4) is given in (24) [2], [14]. The *dq*0 transformed circuit of matrix switches set is shown in Figure 6(f).

$$\mathbf{u}_{Ldq0}=\mathbf{K}_L\mathbf{u}_{Labc}=\mathbf{K}_L\mathbf{M}\mathbf{u}_{SABC}=\mathbf{K}_L\mathbf{M}\mathbf{K}_S^{-1}\mathbf{u}_{Sdq0}=\mathbf{M}_{dq0}\mathbf{u}_{Sdq0}=D_S\begin{bmatrix}q & 0 & 0\\ 0 & q & 0\\ 0 & 0 & 1\end{bmatrix}\mathbf{u}_{Sdq0} \quad (24)$$

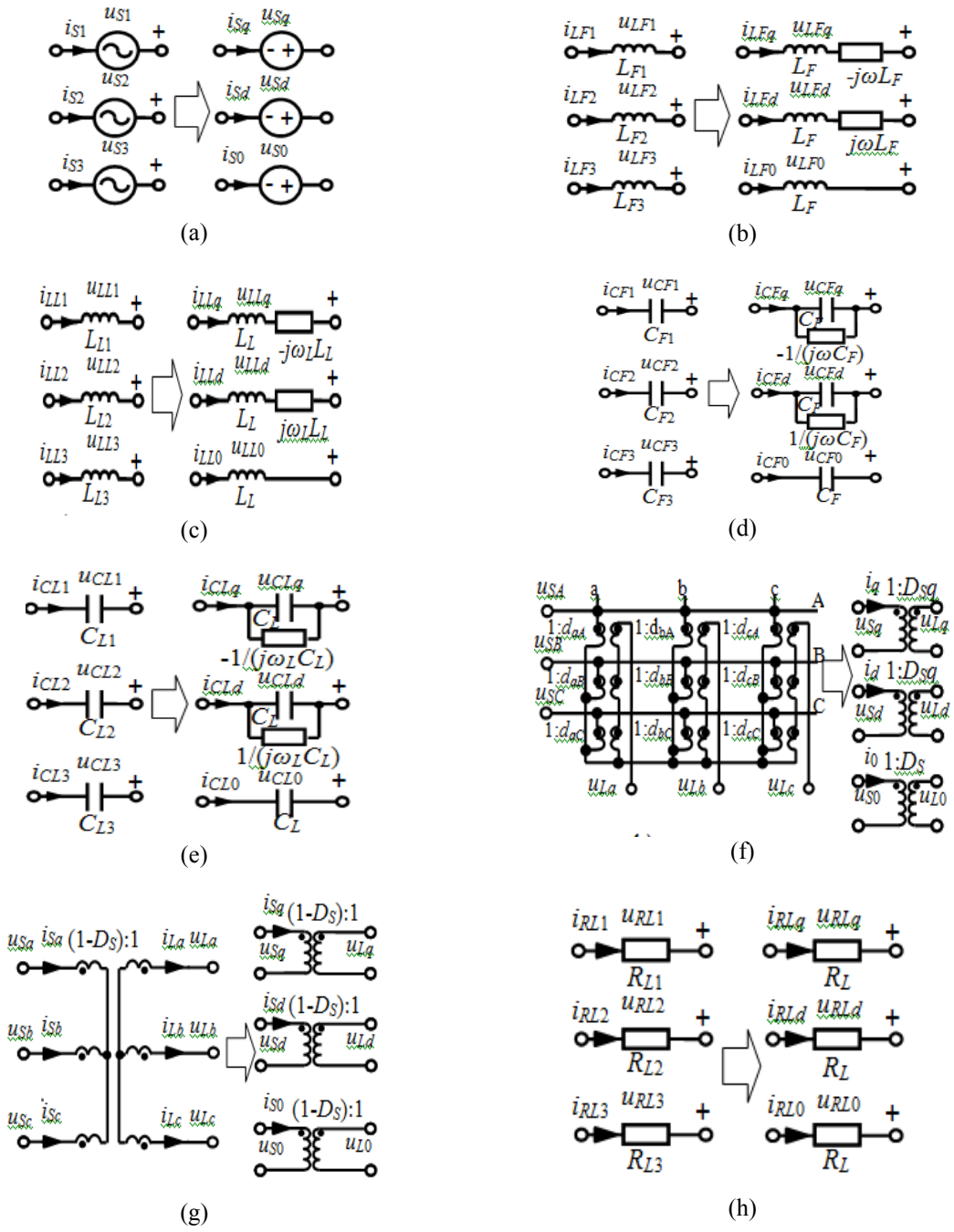

Figure 6. The dq0 transformation of: a) voltage sources, b) source inductors, c) load inductors, d) source capacitors, e) load capacitors, f) matrix switches, g) load switches, h) load resistors

If the switching function of the load switches (Part 6) is defined as:

$$\mathbf{M}_L = \begin{bmatrix} (1-D_S) & 0 & 0 \\ 0 & (1-D_S) & 0 \\ 0 & 0 & (1-D_S) \end{bmatrix} \tag{25}$$

Then the *dq*0 transform is described as follows (Figure 6(g)):

$$\mathbf{u}_{Sabc} = \mathbf{M}_L \mathbf{u}_{Labc} \Rightarrow \mathbf{K}_L^{-1}\mathbf{u}_{Sdq0} = \mathbf{M}_L \mathbf{K}_L^{-1}\mathbf{u}_{Ldq0} \Rightarrow \mathbf{u}_{Sdq0} = \mathbf{M}_L \mathbf{u}_{Ldq0} \tag{26}$$

Assuming that, $R_{L1}=R_{L2}=R_{L3}=R_L$, the procedure of *dq*0 transform of the resistor set (Part 8) is as follows (Figure 6(h)):

$$\mathbf{u}_{Ldq0} = \mathbf{K}_L \mathbf{u}_{Labc} = \mathbf{K}_L R_L \mathbf{i}_{Labc} = R_L \mathbf{i}_{Ldq0} . \tag{27}$$

3.1.3. Circuit Reconstruction

The equivalent *dq*0 circuit models of the presented MRFC (Figure 1) are obtained as shown in Figure 7 by rejoining of the *dq*0 transformed subcircuits. Therefore, the three-phase circuit in Figure 1 can be represented by three single-phase subcircuits for forward, backward and zero-sequence components. Furthermore, assuming that the initial phase of input voltages equals zero $\varphi_1=0$ and that the circuit is symmetrical and balanced, we obtain [2]:

$$\mathbf{u}_{Sdq0} = \mathbf{K}_S \mathbf{u}_S = U_S \begin{bmatrix} 0 \\ 1 \\ 0 \end{bmatrix}. \tag{28}$$

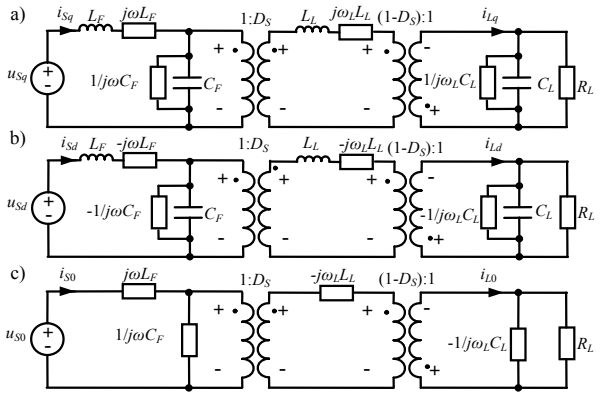

Figure 7. The dq0 transformation of three phase MRFC-I-buck-boost (Figure 1): a) forward sequence component, b) backward sequence component, c) zero-sequence component

The equivalent circuits have been simplified from three circuits to one circuit, which is shown in Figure 8.

3.1.4. Steady State Analysis

There are several analytical methods of analysis averaged models from Figure 8. One of them is a four terminal network theory [17], to steady state circuit analysis. Then, the steady state model is obtained simply by eliminating the reactive elements. Fig.ure 9 shows the steady state model, where all inductors seem to be short and all capacitors open. The steady state characteristics can be obtained by considering the circuit model of the presented MRFC.

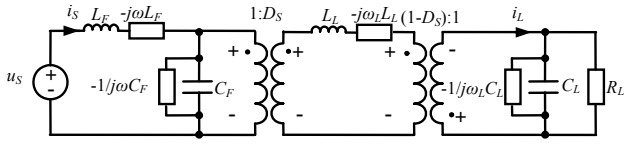

Figure 8. The *dq*0 transformation of three phase MRFC-I-buck-boost MRC (Figure 1) for φ_1=0, and balanced-symmetrical circuit condition

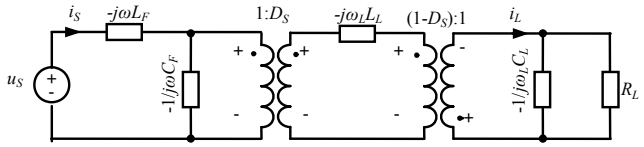

Figure 9. Steady state equivalent circuit of analysed circuit

3.2. State-space Averaging Technique

The general form of the average state space equations is described by following set of equations [12], [15], [16], [18]:

$$\frac{d\overline{\mathbf{x}}}{dt} = \mathbf{A}(d)\overline{\mathbf{x}} + \mathbf{B}(d), \tag{29}$$

where: $\overline{\mathbf{x}}$ is the vector of the averaged state variables, $\mathbf{A}(d)$ and $\mathbf{B}(d)$ are the averaged state matrix and averaged input matrix respectively, d is the continuous duty factor defined by (8). The state-space averaging method is based on analytical manipulations using the different converter state representations [12], [15], [17]. The average state space method applied to the matrix-reactance frequency converter in Fig. 1, is illustrated in Figure 10 by block diagram [12]:

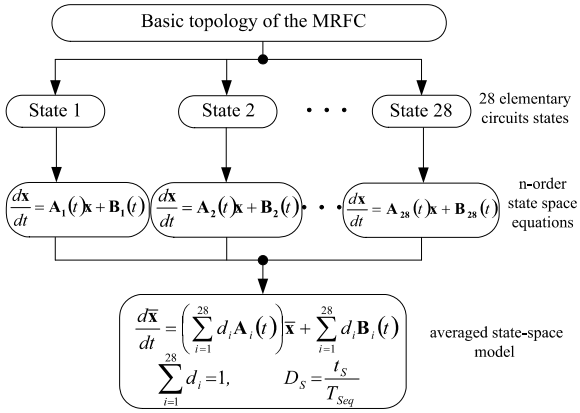

Figure 10. Diagrammatic representation of the state space averaging method for MRFCs

This modelling technique consists in determining, firstly, the linear state model for each possible configuration of the circuit and, then, to combine all these elementary models into a single and unified one through a d_k duty factor. The inputs for the modelling algorithm are all elementary subcircuits for allowed switch state combinations (Figure 10). In all topologies of MRFCs, 28 switch states can be used. Then there are defined differential equations for each of the 28 switch configurations [12]:

$$\frac{d\mathbf{x}}{dt} = \mathbf{A}_k(t)\mathbf{x} + \mathbf{B}_k(t), \tag{30}$$

Where: $\mathbf{x}$ are the vectors of the state variables; $\mathbf{A}_k(t)$ and $\mathbf{B}_k(t)$ are the state matrix and input matrix for *k-th*

switch configuration respectively. The average state space equations for a MRFC can be represented by the following equation [15], [18]:

$$\frac{d\overline{\mathbf{x}}}{dt} = \mathbf{A}(d,t)\overline{\mathbf{x}} + \mathbf{B}(d,t), \tag{31}$$

and $\sum_{k=1}^{28} d_k = 1$, $\mathbf{A}(d,t) = \sum_{k=1}^{28} d_k \mathbf{A}_k(d,t)$, $\mathbf{B}(d,t) = \sum_{k=1}^{28} d_k \mathbf{B}_k(d,t)$.

The weight coefficient d_k is the degree of occurrence of all the possible configurations, and depends on the switch control strategy. Not all 28 switch configurations occur in each switch sequence period T_{Seq}. Equation (31) define the general form of the mathematical average state space model for MRFCs for various control strategies [18], [19].

The mathematical model, of the analysed MRFC (Figure 1), described by the matrix differential equation (31) for Venturini control strategy (4)-(7) is defined as (32) [15]. The model defined by equation (32) is time-varying model in state-space form, because the pulse duty factors d_k for MRFCs is a time variable [12]. A reduced time-invariant model of the MRFC can be found by expressing Equation (32) in the *d-q* rotating frame using the two frequency transformation matrix (9)-(12) [15], [16]. Then, we obtain stationary time-invariant set Equation (33). A detailed matrix description for equations (33) are presented in reference [12].

$$\begin{bmatrix} \frac{d\bar{i}_{S1}}{dt} \\ \frac{d\bar{i}_{S2}}{dt} \\ \frac{d\bar{i}_{S3}}{dt} \\ \frac{d\bar{i}_{LS1}}{dt} \\ \frac{d\bar{i}_{LS2}}{dt} \\ \frac{d\bar{i}_{LS3}}{dt} \\ \frac{d\bar{u}_{CF1}}{dt} \\ \frac{d\bar{u}_{CF2}}{dt} \\ \frac{d\bar{u}_{CF3}}{dt} \\ \frac{d\bar{u}_{L1}}{dt} \\ \frac{d\bar{u}_{L2}}{dt} \\ \frac{d\bar{u}_{L3}}{dt} \end{bmatrix} = \begin{bmatrix} 0 & 0 & 0 & 0 & 0 & 0 & -\frac{1}{L_{F1}} & 0 & 0 & 0 & 0 & 0 \\ 0 & 0 & 0 & 0 & 0 & 0 & 0 & -\frac{1}{L_{F2}} & 0 & 0 & 0 & 0 \\ 0 & 0 & 0 & 0 & 0 & 0 & 0 & 0 & -\frac{1}{L_{F3}} & 0 & 0 & 0 \\ 0 & 0 & 0 & 0 & 0 & 0 & \frac{d_{aA}}{L_{L1}} & \frac{d_{aB}}{L_{L1}} & \frac{d_{aC}}{L_{L1}} & \frac{1-D_S}{L_{L1}} & 0 & 0 \\ 0 & 0 & 0 & 0 & 0 & 0 & \frac{d_{bA}}{L_{L2}} & \frac{d_{bB}}{L_{L2}} & \frac{d_{bC}}{L_{L2}} & 0 & \frac{1-D_S}{L_{L2}} & 0 \\ 0 & 0 & 0 & 0 & 0 & 0 & \frac{d_{cA}}{L_{L3}} & \frac{d_{cB}}{L_{L3}} & \frac{d_{cC}}{L_{L3}} & 0 & 0 & \frac{1-D_S}{L_{L3}} \\ \frac{1}{C_{F1}} & 0 & 0 & -\frac{d_{aA}}{C_{F1}} & -\frac{d_{bA}}{C_{F1}} & -\frac{d_{cA}}{C_{F1}} & 0 & 0 & 0 & 0 & 0 & 0 \\ 0 & \frac{1}{C_{F2}} & 0 & -\frac{d_{aB}}{C_{F2}} & -\frac{d_{bB}}{C_{F2}} & -\frac{d_{cB}}{C_{F2}} & 0 & 0 & 0 & 0 & 0 & 0 \\ 0 & 0 & \frac{1}{C_{F3}} & -\frac{d_{aC}}{C_{F3}} & -\frac{d_{bC}}{C_{F3}} & -\frac{d_{cC}}{C_{F3}} & 0 & 0 & 0 & 0 & 0 & 0 \\ 0 & 0 & 0 & -\frac{1-D_S}{C_{L1}} & 0 & 0 & 0 & 0 & 0 & \frac{-1}{R_{L1}C_{L1}} & 0 & 0 \\ 0 & 0 & 0 & 0 & -\frac{1-D_S}{C_{L2}} & 0 & 0 & 0 & 0 & 0 & \frac{-1}{R_{L2}C_{L2}} & 0 \\ 0 & 0 & 0 & 0 & 0 & -\frac{1-D_S}{C_{L3}} & 0 & 0 & 0 & 0 & 0 & \frac{-1}{R_{L3}C_{L3}} \end{bmatrix} \begin{bmatrix} \bar{i}_{S1} \\ \bar{i}_{S2} \\ \bar{i}_{S3} \\ \bar{i}_{LS1} \\ \bar{i}_{LS2} \\ \bar{i}_{LS3} \\ \bar{u}_{CF1} \\ \bar{u}_{CF2} \\ \bar{u}_{CF3} \\ \bar{u}_{L1} \\ \bar{u}_{L2} \\ \bar{u}_{L3} \end{bmatrix} + \begin{bmatrix} u_{S1} \\ u_{S2} \\ u_{S2} \\ 0 \\ 0 \\ 0 \\ 0 \\ 0 \\ 0 \\ 0 \\ 0 \\ 0 \end{bmatrix} \tag{32}$$

$$\frac{d\mathbf{X}_{dq0}}{dt} = \mathbf{A}\mathbf{X}_{dq0} + \mathbf{B}, \tag{33}$$

The solution of the Equation (33) is described by (34) [12], [15], [16]:

$$\overline{\mathbf{x}} = \mathbf{K}e^{\mathbf{A}t}\mathbf{Y}_{dq0}(0) + \mathbf{K}\mathbf{A}^{-1}\left(e^{\mathbf{A}t} - \mathbf{I}\right)\mathbf{B}, \tag{34}$$

Where: $\mathbf{Y}_{qd0}(0)$–vector of the initial values of transformed variables, **I**–unit matrix. The steady-state values of the averaged state variables from (34) are described by (35) [12], [15], [16].

$$\overline{\mathbf{x}} = -\mathbf{K}\mathbf{A}^{-1}\mathbf{B}. \tag{35}$$

The steady state characteristic of the MRFC topology given in Figure 1 can be analyzed with the help of the solution of average differential Equation (35) [12].

4. VALIDATION OF AVERAGE MODELS

Validation of the obtained model is presented in this section for the parameters summarized in Table 1. Investigations that show the properties of the described MRFC were carried out on a system consisting of a resistance load and the idealized power stage elements.

Using the both obtained models the steady state characteristics and time waveforms are obtained. The results obtained from models based on circuit averaging technique (32)-(34) and models based on state-space averaging technique (35) are the same, and are shown in Figure 11 and Figure 12, [12], [14], [15]. Those figures shown steady state characteristics of the voltage gain (Figure 11) and input power factor (Figure 12) as functions of load voltage setting frequency and sequence pulse duty factor D_S.

Table 1. Calculation test circuit parameters

Parameter	Symbol	Value
Supply voltage	U_S/f	230 V/ 50 Hz
Inductances	L_F and L_L	1.5 mH
Capacitances	C_F and C_L	10 µF

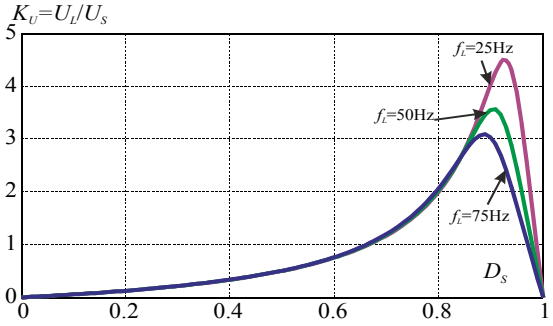

Figure 11. The static characteristics of MRFCs voltage gain as a function of the sequence duty factor D_S for different setting frequencies of the load voltage

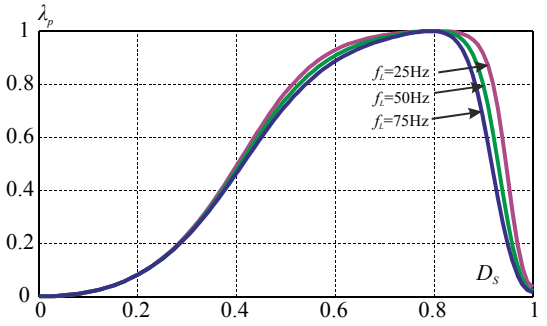

Figure 12. The static characteristics of MRFCs input power factor as a function of the sequence duty factor D_S for different setting frequencies of the load voltage

4. COMPARISON OF PRESENTED MODELLING TECHNIQUES

Table 2. Comparison of the modelling technique

Properties	**Circuit averaging technique**	**State-space averaging technique**
Direct analysis of the circuit scheme	No	Yes
Equivalent schemes	required	Not required
Number of circuit transforming	High	Not required
*dq*0 transformation	required	required
Number of mathematical transformations	High	Medium
The complexity of the mathematical tools	Low	High
Steady state analysis	Yes	Yes
Transient state analysis	Yes, with additional model conversion[1]	Yes, directly
Solution in the form of transmittance	Yes	No
Solution in the time domain	Yes	Yes
Transparency of results	easy to analyze	difficult to analyze
The complexity of the modelling process	High	Low

[1]The transient state analysis with circuit averaging technique are not showed in this paper. The examples transient state modelling are presented in reference [12]

Both modelling techniques have been compared. The results are listed in Table 2. The determination of mathematical averaged state-space models of MRFCs in the presented way is a simple task, which requires only a mathematical transformation without any circuit transformation [15]-[16], [18]. In contrast, the modelling technique based on circuit averaging technique, requires a large number of simple mathematical transformation, and main circuit transformation to equivalent circuit [14]. However, as a result of the modelling using circuit averaging technique, we obtain the results in the form of relatively simple transmittance $H(s)$, while for the state-space averaging technique we obtain results in the complex form of

the time relationship of voltage or current signals – $i(t)$ or $u(t)$. Results in the form of transmittance $H(s)$, from a practical point of view, they are easier to analyze and have many practical implications. However, to obtain results in the form of transmittance $H(s)$ requires a much larger number of circuit and mathematical transformations (Table 2). The time domain equations obtained for state-space averaging technique are difficult to direct analysis and they are used only to graphically demonstrate the properties of a analysed circuit. On the basis of the time waveforms is possibility to obtained indirectly a static characteristics as is shown in Figure 11 and 12.

Both modelling approach can be used to modelling of direct frecuency converters with different number of intput/output phases [20] and different loads [19], [21]

5. CONCLUSION

This paper presents a comparative study of two modelling techniques commonly used for modelling of AC-AC frequency converters. Presented techniques are applied to a AC-AC frequency converter called matrix-reactance frequency converter based on buck-boost topology. The first modulation is based on circuit averaging technique, whereas the second on state-space averaging technique. The obtained models are a key tool in the study of low frequency properties, loadability margins, and control algorithm behavior in presented novel converter, which are presented in previously work [12], [14], [15], [18]. As a main achievement of the paper is to show the differences in the results of two analyzed modelling methods.

The modelling approach based on the averaged state space method presented in this paper is relatively simple and requires only a small number of mathematical transformations. The averaged set equation is obtained directly from the three-phase schematic circuit, taking into account the sequences of switching patterns and modulation strategies (e.g. Venturini). The difficulty in this description stems from the quite complicated analytic solutions. However, the dynamic development of computer systems and mathematical software contribute to the formation of many advanced tools which bring new perspectives to the solution of mathematical problems in the symbolic and numerical approach.

The modelling approach based on the circuit averaging technique is relatively complex and requires a high number of simple mathematical transformations and circuit transformation to single phase equivalent model. However, the obtained results are in the form of relatively simple transmission $H(s)$ which have many practical implications.

ACKNOWLEDGEMENTS

The project has been funded by the National Science Centre granted on the basis of decision number DEC-2011/03/B/ST8/06214

REFERENCES

[1] RD Middlebrook, S Ćuk, *A general unified approach to modelling switching-converter power stages*, Power Electronics Specialists Conference, Cleveland, 1976; 73–86.
[2] CT Rim, *et al.* Transformers as equivalent circuits for switches: general proofs and D-Q transformation-based analyses, *IEEE Transactions on Industrial Application*. 1990; 26(4): 777–785.
[3] J Chen, DT Ngo, Graphical phasor analysis of three-phase PWM converters, *IEEE Transaction on Power Electronics*, 2001; 16(5): 659–666.
[4] D Maksimovic, *et al.*, *Modeling and simulation of power electronic converters*, Proc. of IEEE, 2001; 89(6): 898–912.
[5] HY Kanaan, K Al-Hadad, *A comparison between three modeling approaches for computer implementation of high-fixed-switching-frequency power converters operating in a continuous mode*, Canadian Conference on Electrical and Computer Engineering, Winnipeg, Canada, 2002; 12–15.
[6] CT Rim, Unified general phasor transformation for AC converters, *IEEE Transaction on Power Electronics*, 2011; 26(9): 2465–2475.
[7] JW Kolar, *et al.* Novel three-phase AC-DC-AC sparse matrix converter, *IEEE Applied Power Electronics Conference and Exposition,* Dallas, 2002; 2: 777–791.
[8] JW Kolar, *et al. The essence of three-phase AC/AC converter systems*, Power Electronics and Motion Control Conference, Poznań, Poland, 2008; 27–42.
[9] JW Kolar, *et al.* Review of three-phase PWM AC–AC converter topologies, *IEEE Transaction on Industrial Electronics*, 2011; 58(11): 4988–5006.
[10] Z Fedyczak, *et al. New family of matrix-reactance frequency converters based on unipolar PWM AC matrix-reactance choppers*, Power Electronics and Motion Control Conference*,* Poznań, Poland, 2008; 236–243.
[11] K Koiwa, Ji Itoh, *Experimental verification for a matrix converter with a V connection AC chopper*, European Conference on Power Electronics and Applications, Birmingham, UK, 2011; 1–10.

[12] P Szcześniak, Three-phase AC-AC Power Converters Based on Matrix Converter Topology. *Matrix-Reactance Frequency Converters Concept*, Berlin-Heidelberg, Springer, 2013.
[13] J Rodriguez, *et al.*, A review of control and modulation methods for matrix converters, *IEEE Transaction on Industrial Electronics*, 2012; 59(1): 58–70.
[14] P Szcześniak, *et al.*, *Modeling and analysis of a matrix-reactance frequency converter based on buck–boost topology by DQ0 transformation*, Power Electronics and Motion Control Conference, Poznań, Poland, 2008; 165–172.
[15] Z Fedyczak, P Szcześniak, Matrix-reactance frequency converters using an low frequency transfer matrix modulation method, *Electric Power System Research*, 2012; 83: 91–103.
[16] I Korotyeyev, Z. Fedyczak, Steady and transient states modelling methods of matrix-reactance frequency converter with buck-boost topology, *COMPEL–Int. J. Comput. Math. Electr. Electron. Eng.*, 2008; 28(3): 626–638.
[17] Z Fedyczak, Four-terminal chain parameters of averaged AC models of non-isolated matrix-reactance PWM AC line conditioners, *Archives of Electrical Engineering*, 2001; 50(4): 395–409.
[18] P Szcześniak, A static and dynamic model of a space vector modulated matrix-reactance frequency converter, *Electric Power System Research*, 2014; 108: 82–92.
[19] CSA Sekhar, *et al.*, Space Vector Modulation Based Direct Matrix Converter for Stand-Alone system, *International Journal of Power Electronics and Drive Systems (IJPEDS)*, 2014; 4(1): 24-35.
[20] Sk M Ahmed, *et al.*, Carrier Based Pulse Width Modulation Control of a Non-Square Direct Matrix Converter with Seven-phase Input and Three-phase Output, *International Journal of Power Electronics and Drive Systems (IJPEDS)*, 2013; 3(3): 344-350.
[21] F Safargholi, Unity Power Factor at the Power Supply Side for Matrix Converter Fed PMSM Drives, *International Journal of Electrical and Computer Engineering (IJECE)*, 2014; 4(1): 138-144.

BIBLIOGRAPHY OF AUTHOR

Pawel Szczesniak received the M.Sc. and Ph.D. degrees in electrical engineering from the University of Zielona Gora, Zielona Gora, Poland. He is currently a Researcher with the Institute of Electrical Engineering, University of Zielona Gora. His research focuses mainly on power electronics systems in power network, particularly the analysis, modelling and study of properties of AC/AC converters without DC energy storage.